Cumhuriyet Sci. J., 45(2) (2024) 400-406
DOI: https://doi.org/10.17776/csj.1441702

Cumhuriyet Science Journal

| csj.cumhuriyet.edu.tr | Founded: 2002 ISSN: 2587-2680 e-ISSN: 2587-246X Publisher: Sivas Cumhuriyet University

A Study on the Growth Conditions Role in Defining InGaAs Epitaxial Layer Quality

Meryem Demir [1,a,*], Sezai Elagöz [2,b]

[1] *Aselsan Sivas Precision Optics, 58060, Sivas, Türkiye.*
[2] *Nanophotonics Research and Application Center, Sivas Cumhuriyet University, 58140, Sivas, Türkiye.*
**Corresponding author*

Research Article

History
Received: 22/02/2024
Accepted: 11/03/2024

This article is licensed under a Creative Commons Attribution-NonCommercial 4.0 International License (CC BY-NC 4.0)

ABSTRACT

This study delves into the epitaxial growth and characterization of $In_xGa_{1-x}As$ layers on InP substrate, a critical area in the development of high-performance III-V semiconductor devices. $In_xGa_{1-x}As$ is renowned for its superior electron mobility and broad spectral response, making it indispensable in applications ranging from photodetectors to quantum cascade lasers. Employing a horizontal flow reactor MOVPE (metal-organic vapor phase epitaxy) technique, we meticulously grew n-$In_xGa_{1-x}As$ epilayers under varying conditions to investigate the impact of indium content, growth temperature, and V/III ratio on the material's structural, optical, and electrical properties. HRXRD (High-resolution X-ray diffraction) and Hall-effect measurements provided insights into the correlation between growth parameters and epitaxial layer quality, including dislocation density and carrier mobility. Our findings highlight the delicate balance required in the growth process to optimize the $In_xGa_{1-x}As$ /InP structure's performance for advanced semiconductor applications. The research underscores the potential of tailored $In_xGa_{1-x}As$ layers to push the boundaries of current photonics and optoelectronics technologies, emphasizing the importance of growth condition optimization for enhancing device efficiency and thermal stability.

Keywords: $In_xGa_{1-x}As$, Epitaxy, Growth, Indium

[a] mdemir@aho.com.tr
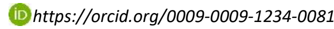
https://orcid.org/0009-0009-1234-0081
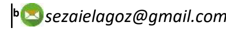
[b] sezaielagoz@gmail.com
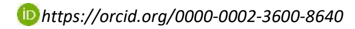
https://orcid.org/0000-0002-3600-8640

Introduction

In the realm of semiconductor materials, Indium Gallium Arsenide ($In_xGa_{1-x}As$) stands out as a pivotal III-V compound, renowned for its exceptional electron mobility and saturation shift rate [1]. This material has carved a niche in various high-tech applications, ranging from remote sensing and environmental monitoring to fiber optic communication and short-wave infrared photodetectors [2-7]. The ability of $In_xGa_{1-x}As$ -based devices to cater to wavelengths within the 0.85–3.60 µm spectral range is a testament to its versatility and technological importance [8]. A critical aspect of $In_xGa_{1-x}As$'s utility lies in its lattice-matched structure with Indium Phosphide (InP), which has been the subject of extensive investigation. Despite certain drawbacks of the InP substrate, such as its relative fragility and higher cost compared to Gallium Arsenide (GaAs) substrates, its electrical properties and reduced lattice mismatch make it theoretically more suitable for base material in certain applications. InP substrates have demonstrated promising performance, especially in the 0.9-1.6µm wavelength region, encompassing a range of applications from photodetectors to photodiodes [9-14]. The evolution of epitaxial growth technologies, including Molecular Beam Epitaxy (MBE), Solid Phase Epitaxy (SPE), Physical Vapor Deposition (PVD), and Metal Organic Vapor Phase Epitaxy (MOVPE), has been a cornerstone in achieving high-performance semiconductor thin films. MOVPE, in particular, has gained prominence since 1968 for its ability to produce high-quality crystal layers at a remarkable growth rate, making it fit for large-scale production [15]. The growth parameters such as substrate temperature, pressure of growth chamber, reactants quantity, semiconductor-alloy-composition, and group V/group III play a pivotal part in defining the characteristics of $In_xGa_{1-x}As$ epitaxial layers [16-21]. The variation of indium concentration in the $In_xGa_{1-x}As$ alloy is a critical factor affecting the crystal quality and optical properties. Studies have shown that increasing indium concentration can lead to greater lattice mismatch and pit dislocation density [22-23]. This variation also impacts the refractive index, as observed in spectroscopic ellipsometry measurements [24]. Additionally, research into the structural and electrical attributes of $In_xGa_{1-x}As$/InP compositions has highlighted the importance of the indium alloy mix and the metal layering process at ambient temperature [8]. Another pivotal aspect of $In_xGa_{1-x}As$ is its energy bandgap, which falls in from the near-infrared to mid-infrared wavelength range. This feature renders $In_xGa_{1-x}As$ a suitable material for infrared device applications. Understanding and optimizing the energy bandgap is crucial for developing detectors with desired properties, including optimal thickness, refractive index, and optical reflection/transmission. The wider range of $In_xGa_{1-x}As$ uses encompasses uncooled infrared sensors, light-emitting devices, field-effect-transistors, and quantum cascade lasers [3, 25-27]. The performance of these

devices is intricately linked to the quality of the $In_xGa_{1-x}As$ layers, influenced by growth conditions and parameters such as growth temperature, rate, and V/III ratio. Carrier localization in In-doped structures is a notable phenomenon, especially in the context of $In_xGa_{1-x}As$ alloys [18]. This aspect is significant due to the compositional inhomogeneity induced by high Indium content and the presence of In-related impurities. The localization effect is observed in various III-V alloys and is manifested in features like temperature-dependent photoluminescence [19]. Theoretical models have been developed to interpret and simulate these phenomena, contributing to a deeper understanding of the optical behavior of these materials.

In this research, the impact of various growth environments on Metalorganic Vapor Phase Epitaxy (MOVPE)-grown $In_xGa_{1-x}As$ epilayers is examined. Techniques such as X-ray diffraction (XRD), in-situ optical reflectivity, and room-temperature Hall-effect measurements are employed to assess the distinct growth conditions of $In_xGa_{1-x}As$ epilayers.

Experimental

In this study, n-InxGa1-xAs epilayers were grown utilizing a state-of-the-art crystal growth system, Aixtron 200/4 RF-S horizontal flow reactor MOCVD system. Epitaxial layers were deposited on 2-inch, (100)-oriented, semi-insulating, double-side polished (dsp) indium phosphide (SI-InP) substrates. The epitaxial growths were achieved at 680 °C. A variety of InxGa1-xAs layers were developed, with thicknesses ranging from 500 to 1000 nm, and varying indium contents (from x = 0.529 to 0.532). Uniform layers in terms of thickness and composition were ensured through gas flow rotation. The group-III precursors used were opto-grade trimethylgallium (TMGa) and trimethylindium (TMIn), while the group-V precursors were high-purity arsine (AsH3) and phosphine (PH3). Silane (SiH4) was employed for n-type doping. The carrier gases used included ultra-highly purified hydrogen (H2) and nitrogen (N2). Growth parameters were meticulously controlled, with reactor temperatures set 680 °C, and reactor pressure maintained at 50 mbar. The AsH3 flow rates varied across different two samples, altering the V/III ratios. Additionally, an InP buffer layer of approximately 500 nm was grown prior to each InxGa1-xAs layer to enhance material quality. For real-time monitoring of growth rate, reflection intensity, and surface quality, a Luxtron 880 nm reflectometer and optical fiber thermometry-light-pipe assembly were incorporated. The MOVPE system was also equipped with a rotating susceptor for substrate rotation, optimizing the epitaxial layer quality.

Structural analysis was carried out using High-Resolution X-Ray Diffraction (HRXRD) on a Rigaku SmartLab diffractometer, which is equipped with a rotating Cu anode and a four-bounce Ge (220) monochromator. The electrical characteristics, such as sheet carrier concentration, mobility, and resistivity, were assessed using a Hall-effect measurement system (HEMS), utilizing the four-probe Van der Pauw method. This thorough methodology facilitated an in-depth exploration of the structural, optical, and electrical attributes of the InxGa1-xAs epilayers. It offered valuable insights into how various growth conditions influence their properties. The growth conditions and parameters for all samples are detailed in Table 1 below.

Table 1. Growth parameters of samples.

Sample	*TMIn (sccm)*	*TMGa (sccm)*	*AsH_3 (sccm)*	*SiH_4 (sccm) s/d/i*	*Growth rate (nm/s)*	*Thickness (nm)*
A	242	9	200	6/400/10	1.32	1000
B	242	9	200	6/350/10	1.33	1000
C	242	9	162	2/500/10	1.43	500

Results and Discussion

On the InP substrate, a buffer layer of InP is first grown, followed by $In_xGa_{1-x}As$ layers for every sample. The in-situ reflectance-temperature graphs of these growths are given by Figure 1, Figure 2, and Figure 3. The blue line in this figure represents the in-situ reflectance intensity and the green one represents the growth temperature of the reactor during the growth. From the in-situ reflectance measurements, it is observed that there are no unwanted conditions on the surface during growth, and also that the surface quality is not degraded during the growth. At the first stage of growth, no interference oscillation is observed in the in-situ reflectance graph since there is no refractive index difference between the InP buffer layer to be grown on the InP substrate and the substrate itself [17]. As shown in Figure 1-Figure 3, after

the successful growth of the InP buffer layer on the InP substrate, doped $In_xGa_{1-x}As$ alloys have been grown.

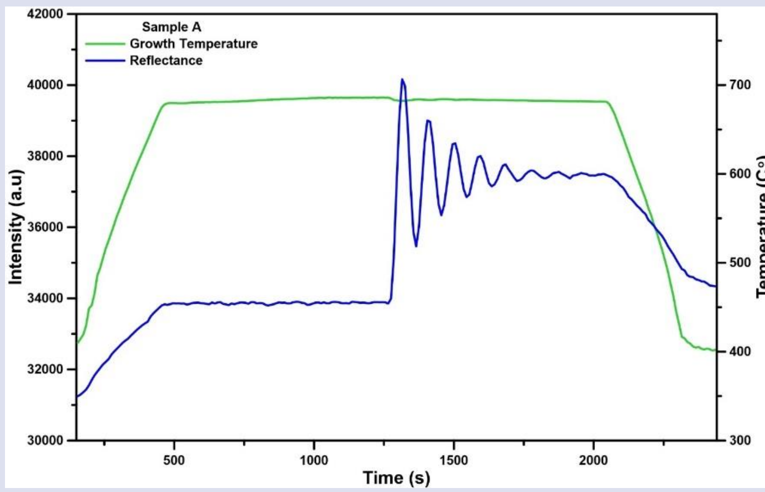

Figure 1. Temperature and in-situ reflectance measurements of sample A.

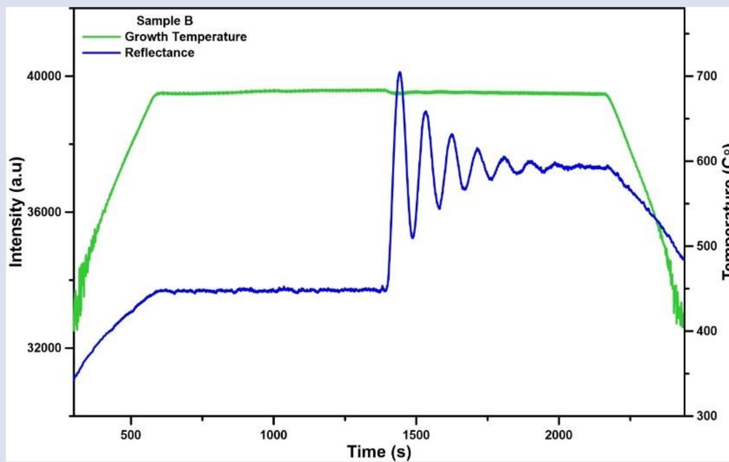

Figure 2. Temperature and in-situ reflectance measurements of sample B.

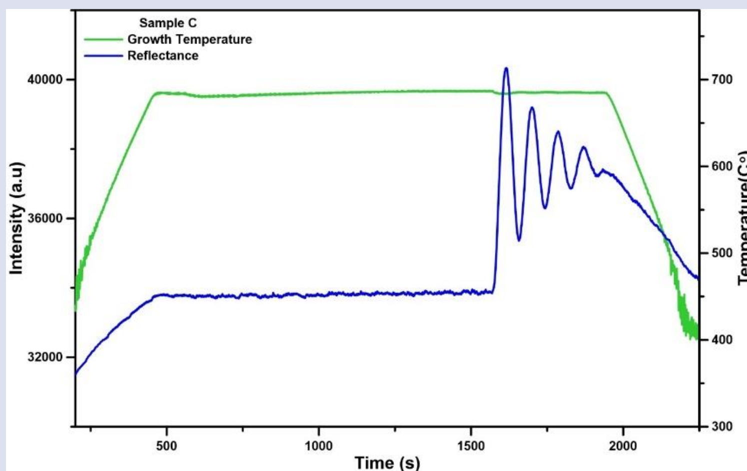

Figure 3. Temperature and in-situ reflectance measurements of sample C.

It was obtained from the in-situ reflectance measurements that the growth rate of sample A, sample B, and sample C are 1.32, 1.33, and 1.43 nm/s, respectively. It can be understood from the comparison of samples A and B that the growth rate is not affected seriously by decreasing the SiH_4 dilute flow which is about the dilution of the SiH_4 precursor. However, it is clear that the growth rate is affected when the AsH_3 flow is changed from 200 sccm to 162 sccm. It is believed that the AsH_3 flow is more effective than the SiH_4 flow considering the growth rate. Literature indicates that an increased presence of AsH_3 in the reactor, or more precisely on the growth surface, results in a reduced growth rate for $In_xGa_{1-x}As$ epitaxial layers [28].

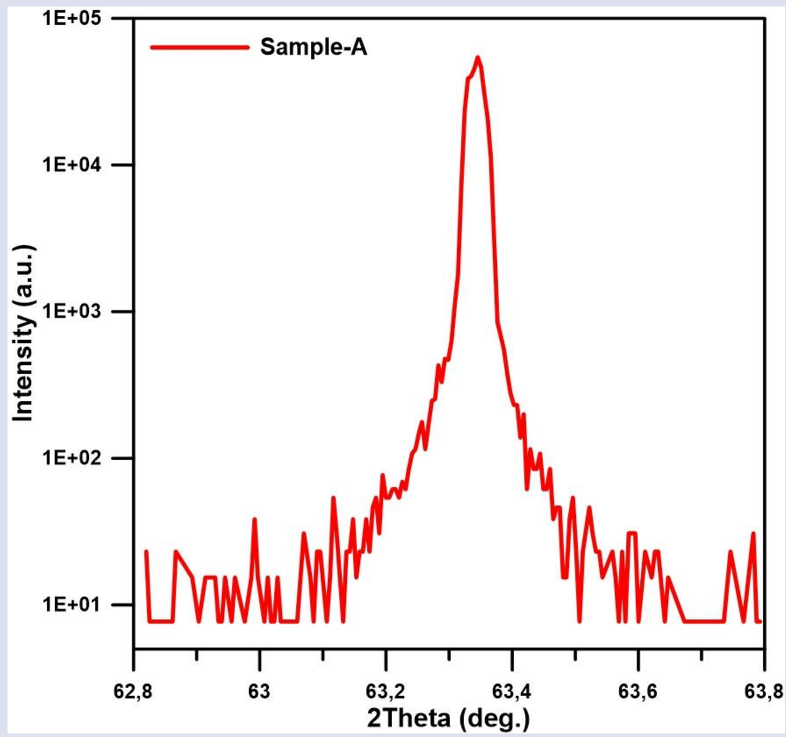

Figure 4. HRXRD measurement of sample A.

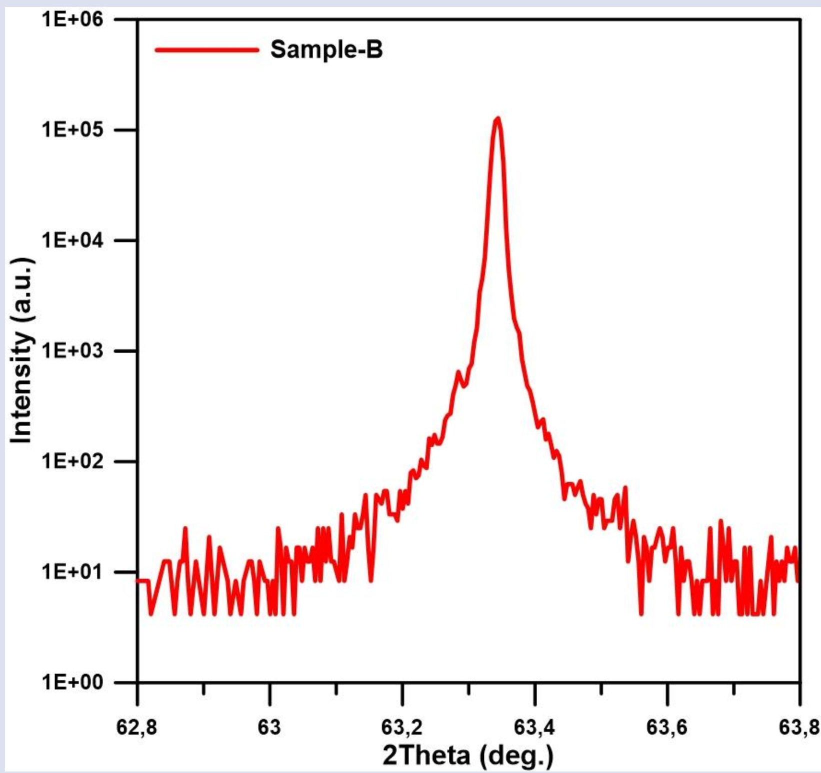

Figure 5. HRXRD measurement of sample B.

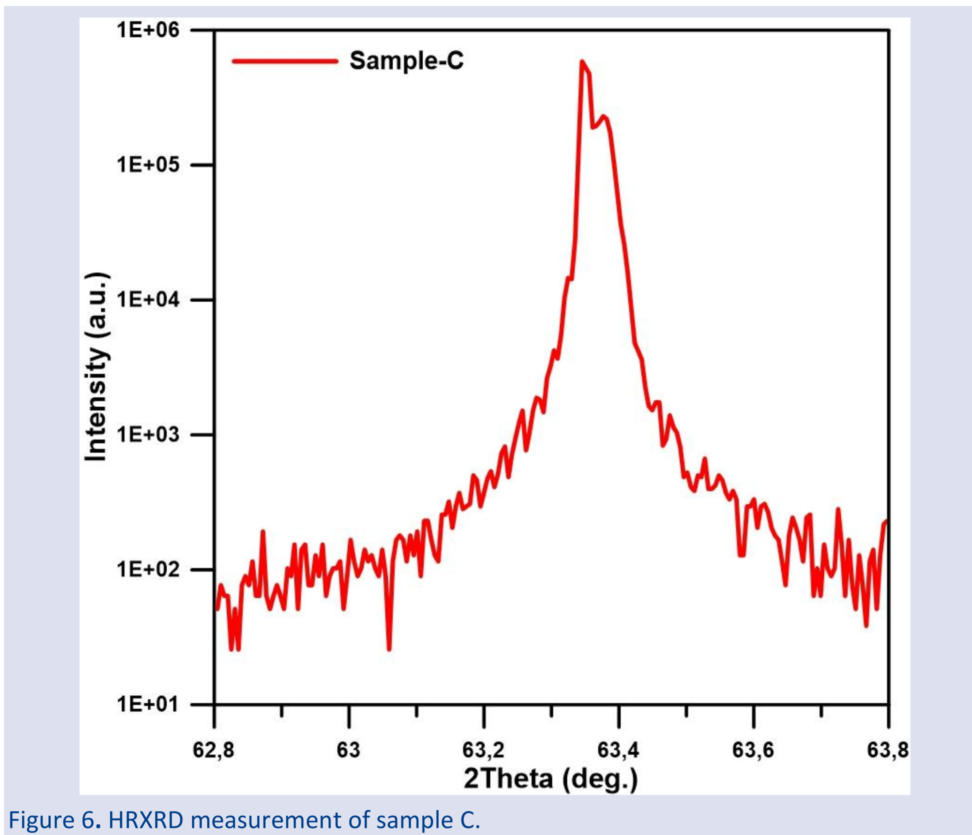

Figure 6. HRXRD measurement of sample C.

XRD is a strong and non-destructive characterization technique to have valuable and detailed information in terms of the alloy concentration, structural properties of epitaxial thin films, and, thickness [24]. The HRXRD 2θ scans of three samples are carried out to investigate the effect of growth conditions. Figure 4, Figure 5, and Figure 6 reveal the HRXRD 2θ patterns of all $In_xGa_{1-x}As$ samples. The selection was made for the interval between 63° and 63.8°, where the (0 0 4) Bragg peaks are situated for both the InP substrate and the $In_xGa_{1-x}As$ epilayer. In this depiction, it is evident that the peaks with the highest intensity and the narrowest Full Width at Half Maximum (FWHM) originated from InP substrates, while the other peaks were attributed to the $In_xGa_{1-x}As$ layers.

When examining the High-Resolution X-Ray Diffraction (HRXRD) scans for samples A, B, and C, it is observed that the $In_xGa_{1-x}As$ peaks are positioned to the left and to the right of the InP substrate peak. This positioning indicates that the $In_xGa_{1-x}As$ epitaxial films are experiencing compressive strain, are lattice-matched, and have tensile strain, which leads to an increase in the out-of-plane lattice parameters. The InAs alloy ratios of the samples, as determined from the measurements and simulations, are 0.533, 0.532, and 0.529 for samples A, B, and C, respectively.

Furthermore, the strain existing between the $In_xGa_{1-x}As$ epitaxial layers and the substrate can be calculated from the HRXRD measurements in the following manner:

$$\frac{\Delta a}{a} = -\frac{\Delta\theta}{\tan(\theta_B)} \quad (1)$$

where Δθ represents the angular difference between the diffraction peaks of the epitaxial $In_xGa_{1-x}As$ layer and the InP substrate, and θ_B is the Bragg angle for the InP substrate. The observation shows that with an increase in indium content and the presence of compressive strain, there is a distinct shift of the Bragg peak toward lower 2θ angles. Furthermore, a greater mismatch between the $In_xGa_{1-x}As$ epilayer and the InP substrate leads to a wider Full Width at Half Maximum (FWHM) of the Bragg peak, despite the film thickness remaining constant. This indicates the emergence of defects, most likely dislocations, which serve to alleviate the misfit strain exerted by the substrate. According to established literature, the density of dislocations (N_{dd}) in epitaxial layers can be estimated using a specific formula, which quantifies the relationship between dislocation density and observed structural characteristics in epitaxial films.

$$N_{dd} = 2 * \frac{(FWHM)^2}{9{a_0}^2} \quad (2)$$

where a_0 is the lattice constant of the $In_xGa_{1-x}As$ epitaxial layer. We then determined here $In_xGa_{1-x}As$ lattice constant is a_0. Based on this, the dislocation density for all samples was determined and is presented in Table 2. Analysis of Table 2 reveals that reducing the indium content, through values of x = 0.533, 0.532, and 0.529 leads to a decrease in lattice constant of $In_xGa_{1-x}As$. The calculated dislocation density values for samples A, B, and C are 2.11, 0.51, and 1.55 (10^9 cm^{-2}), respectively. Notably, the narrowest Full Width at Half Maximum (FWHM) of 58 arcsec was observed for sample B, indicating it has the highest crystalline quality among the samples. Nonetheless, it is evident that all samples exhibit good crystalline quality

Table 2. The HRXRD results of the $In_xGa_{1-x}As$ epitaxial layers

Sample	InAs alloy ratio	Lattice Constant (A)	FWHM (arcsec)	Dislocation Density (10^9 cm^{-2})
A	0.533	5.8674	118	2.11
B	0.532	5.8661	58	0.51
C	0.529	5.8629	101	1.55

Hall effect measurements were performed to explore the impact of varying growth conditions on the electrical properties of the $In_xGa_{1-x}As$ epilayers. This technique allows for the determination of carrier concentration, mobility, and resistivity of the samples, providing valuable insights into how different growth parameters influence the electrical behavior of the fabricated layers. By applying a magnetic field and measuring the voltage generated perpendicular to the current flow, the Hall effect offers a direct method to probe the type and density of charge carriers within a material, as well as their mobility, which are crucial factors in assessing the material's performance for electronic and optoelectronic applications. The net SiH_4 reactant supplied to the reactor is calculated by using the following formula

$$r = i * \frac{s}{s+d} \quad (3)$$

here i is inject, s is source, and d is dilute amount of the mass flow controllers, respectively. So, the net amounts of SiH4 precursors are 0.14, 0.16, and 0.38 µmol/min, respectively. Table 3 shows the room temperature mobility and sheet carrier concentration values of InxGa1-xAs epitaxial layers. Samples A, B, and C have 1.4, 2.0, and 1.9 E+13 cm-2 for sheet carrier concentration and 1.7, 1.5, and 2.4E+4 Vs/cm-2 for mobility, respectively. It is clear from the measurement results that the carrier concentration increases (mobility decreases) of sample B as expected by decreasing the dilution (or increasing the net amount of precursor) of the SiH4 source. It is obtained that even though the SiH4 precursor flow increased more than double, the V/III ratio changes affect the carrier concentration change more than SiH4 amount. As documented in the literature, when the flow rate of arsine (AsH3) is increased during the growth process, there is a significant rise in carrier density alongside a reduction in mobility. This phenomenon is attributed to the enhanced incorporation of arsenic into the material, which can lead to an increase in the number of charge carriers (electrons or holes) within the semiconductor. However, the increased incorporation of arsenic can also introduce additional scattering centers or defects, which adversely affect the mobility of these carriers by impeding their flow through the crystal lattice. Mobility is an essential parameter in semiconductors as it influences how quickly charge carriers can move under the influence of an electric field, impacting the material's electrical conductivity and overall performance in electronic devices [21]. Also, it is known that the effect of the V/III ratio of n-InxGa1-xAs is strong on Si incorporation into the structure [28]. It is thought also that the increase in mobility of sample C can be related to the positive contribution of the AsH3 amount in the reactor.

Table 3. The Hall Effect results of the $In_xGa_{1-x}As$ epitaxial layers.

Sample	Sheet carrier concentration (cm^{-2})	Mobility (Vs/cm^2)
A	1.4E+13	1.7E+4
B	2.0E+13	1.5E+4
C	1.9E+13	2.4E+4

Conclusion

This study has comprehensively explored the properties of $In_xGa_{1-x}As$ epitaxial layers grown on InP substrates, focusing on the impacts of varying growth conditions on the structural, optical, and electrical properties of the layers. Through meticulous experimentation, the research has highlighted the critical role of growth parameters in defining the characteristics of $In_xGa_{1-x}As$ layers, demonstrating how variations in indium content, reactor temperature, and V/III ratio influence layer quality, dislocation density, and carrier mobility. The findings underscore the potential of optimizing $In_xGa_{1-x}As$/InP structures for advanced semiconductor applications, particularly in photodetectors, field-effect transistors, and quantum cascade lasers. Future work should aim at refining growth techniques to further enhance the performance of $In_xGa_{1-x}As$ -based devices, potentially opening new avenues for the application of III-V semiconductors in optoelectronics and photonics, where efficiency, speed, and thermal stability are paramount.

Conflicts of interest

There are no conflicts of interest in this work.

Acknowledge

The authors acknowledge the usage of the Nanophotonics Research and Application Center at Sivas Cumhuriyet University (CUNAM) facilities.

References

[1] Nee T.W., Green, A.K., Optical properties of InGaAs lattice-matched to InP, *J. Appl. Phys.*, 68 (10) (1990) 5314-5317.

[2] Zhao L., Guo Z., Wei Q., Miao Q., Zhao L., The relationship between the dislocations and microstructure in In0.82Ga0.18As/InP heterostructures, *Sci. Rep.*, 6 (1) (2016) 1-7.

[3] Smiri B., Arbia M.B., Demir I., Saidi F., Othmen Z., Dkhil B., Altuntas I., Elagoz S., Hassen F., Maaref H., Optical and structural properties of In-rich InxGa1− xAs epitaxial layers on (1 0 0) InP for SWIR detectors, *Mater. Sci. Eng. B.*, 262 (2020) 114769.

[4] Buckley D. N., The effect of gas phase growth parameters on the composition of InGaAs in the hydride VPE process, *J. Electron. Mater.*, 17 (1) (1988) 15-20.

[5] Vallejo K.D., Cabrera-Perdomo C.I., Garrett T.A., Drake M.D., Liang B., Grossklaus K.A., and Simmonds P.J., Tunable Mid-Infrared Interband Emission from Tensile-Strained InGaAs Quantum Dots, *ACS Nano*, 17 (3) (2023) 2318–2327.

[6] Yan Z., Shi T., Fan Y., Zhou L. and Yuan Z., Compact InGaAs/InP single-photon detector module with ultra-narrowband interference circuits, Advanced Devices & Instrumentation 4, (2023) 0029.

[7] Kalyon G., Mutlu S., Kuruoglu F., Pertikel I., Demir I., Erol A., InGaAs-based Gunn light emitting diode, *Mater. Sci. Semicond. Process* 159, (2023) 107-389.

[8] Asar T., Özçelik S., Özbay E., Structural and electrical characterizations of InxGa1-xAs/InP structures for infrared photodetector applications, *J. Appl. Phys.,* 115 (10) (2014) 104502.

[9] Eckl J. J., Schreiber K. U., Schüler T., Satellite laser ranging in the near-infrared regime, *Photon Counting Applications-SPIE*, (2017) 10229 75-81.

[10] Ma J., Bai B., Wang L.J., Tong C.Z., Jin G., Zhang J., Pan J.W., Design considerations of high-performance InGaAs/InP single-photon avalanche diodes for quantum key distribution, *Appl. Opt.*, 55 (27) (2016) 7497-7502.

[11] Cova S., Ghioni M., Itzler M. A., Bienfang J. C., Restelli A., Semiconductor-based detectors, *Experimental Methods in the Physical Sciences*, 45 (2013) 83-146.

[12] Tosi A., Acerbi F., Dalla Mora A., Itzler M.A., Jiang X., Active area uniformity of InGaAs/InP single-photon avalanche diodes, *IEEE Photonics J.*, 3 (1) (2010) 31-41.

[13] Itzler M.A., Jiang X., Entwistle M., Slomkowski K., Tosi A., Acerbi F., Zappa F. and Cova S., Advances in InGaAsP-based avalanche diode single photon detectors, *J. Mod. Opt.*, 58 (3-4) (2011) 174-200.

[14] Jiang X., Itzler M. A., Ben-Michael R., Slomkowski K., InGaAsP–InP avalanche photodiodes for single photon detection, *IEEE J. Sel. Top. Quantum Electron.,* 13 (4) (2007) 895-905.

[15] Dupuis R.D., III–V semiconductor devices grown by metalorganic chemical vapor deposition—The development of the Swiss Army Knife for semiconductor epitaxial growth, *J. Vac. Sci. Technol. B,* 41 (6) (2023).

[16] Unal D.H., Demir I., InGaAs-Based MSM Photodetector: Researching Absorption Layer, Barrier Layer, and Digital Graded Superlattice Layer with 3D Simulation, *Results Opt.,* 13 (2023) 100581.

[17] Perkitel I., Demir I., Effect of Si-doped and undoped inter-layer transition time on the strain-compensated InGaAs/InAlAs QCL active region grown with MOVPE, *J. Mol. Struct.,* 1272 (2023) 134203.

[18] Arbia M.B., Demir I., Kaur N., Saidi F., Zappa D., Comini E., Altuntaş I. and Maaref H., Experimental insights toward carrier localization in in-rich InGaAs/InP as candidate for SWIR detection: Microstructural analysis combined with optical investigation, *Mater. Sci. Semicond. Process.,* 153 (2023) 107149

[19] Badreddine S., Joshya R.S., Ilkay D., Faouzi S., Ismail A., Lagarde D., Rober C., Xavier M., Hassen M., Systematic optical study of high-x InxGa1-xAs/InP structures for infrared photodetector applications, *Opt. Laser Technol.,* 148 (2022) 107714.

[20] Arbia M.B., Smiri B., Demir I., Saidi F., Altuntas I., Hassen F. and Maaref H., Theoretical analyses of the carrier localization effect on the photoluminescence of In-rich InGaAs layer grown on InP, *Mater. Sci. Semicond. Process.,* 140 (2022) 106411.

[21] Demir I., Altuntas I., and Elagoz S., Arsine flow rate effect on the low growth rate epitaxial InGaAs layers, *Semiconductors* 55 (10) (2021) 816-822.

[22] Alaydın B. O., Tüzemen E. S., Demir I., and Elagöz S., Optical and Structural Properties of MOCVD Grown InxGa1-xAs Epilayers, *Cumhuriyet Sci. J.,* 38 (4) (2017) 681-689.

[23] Gu Y., Huang W., Liu Y., Ma Y., Zhang J., Gong Q., Zhang Y., Shao X., Li X. and Gong H., Effects of buffer doping on the strain relaxation of metamorphic InGaAs photodetector structures, Mater. Sci. Semicond. Process., 120 (2020) 105281.

[24] Kaynar E., Sayrac M., Altuntas I., and Demir I., Determination of Optical Properties of MOVPE-Grown InxGa1-xAs/InP Epitaxial Structures by Spectroscopic Ellipsometry, *Braz. J. Phys.,* 52 (5) (2022) 184.

[25] Demir I., Altuntas I., Bulut B., Ezzedini M., Ergun Y. and Elagoz S., Comprehensive growth and characterization study on highly n-doped InGaAs as a contact layer for quantum cascade laser applications, *Semicond. Sci. Technol.,* 33, (5) (2018) 055005.

[26] Olausson P. and Lind E., Geometrical magnetoresistance as a tool for carrier mobility extraction in InGaAs MOSFETs, *IEEE Trans. Electron Devices,* (2023).

[27] Yang B., Yu Y., Zhang G., Shao X. and Li X., Design and Fabrication of Broadband InGaAs Detectors Integrated with Nanostructures, *Sensors,* 23 (14) (2023) 6556.

[28] Jiang L., Lin T., Wei X., Wang G.H., Zhang,G.Z., Zhang H.B. and Ma X.Y., Effects of V/III ratio on InGaAs and InP grown at low temperature by LP-MOCVD, *J. Cryst. Growth,* 260 (1-2) (2004) 23-27.